Computación y Sistemas Número Especial pp. 099 - 107
© 2002, CIC - IPN. *ISSN 1405-5546* Impreso en México

An Analysis of the Active Layer Optimization of High Power Pulsed IMPATT Diodes

Un Análisis de la Optimización de la Capa Activa de Diodos Pulsados de Alta Potencia Tipo IMPATT

Alexander Zemliak and **Roque De la Cruz Jiménez**
Departamento de Física y Matemáticas , Universidad Autónoma de Puebla, México
E-mails: {azemliak, roquejim}@fcfm.buap.mx

Article received on June 12, 2001; accepted on February 19, 2002

Resumen

En la base del modelo numérico que incluye modelos precisos eléctricos y térmicos, las características extremales de potencia han sido investigadas para el diodo IMPATT de modo pulsado de la región de 94 y 140 GHz. Los diodos con perfil tradicional y perfil complejo fueron optimizados por su estructura interna. La estructura semiconductora compleja ha sido analizada para mejorar las caracteristicas de potencia y eficiencia del diodo IMPATT. Las dependencias de potencia, eficiencia y admitancia han sido investigadas como funciones de la corriente de alimentación. La estructura semiconductora compleja puede ser recomendable para aumentar el tiempo real de trabajo del diodo potente de modo pulsado.

Palabras Clave: Dispositivos Semiconductores de Microondas, Simulación y Modelado, Métodos Numéricos, Optimización de la Estructura.

Abstract

On the basis of numerical model that includes precise electrical and thermal sub-models, the extremely energy characteristics are investigated of a pulsed-mode Si double-drift IMPATT diodes for 94 and 140 GHz. The optimization of the internal structure of the diode with a traditional doping profile and with a complex doping profile is provided. Semiconductor structures with a complex doping profile are analyzed for improving the power level and efficiency of IMPATT diode. The dependencies of power level, efficiency, and admittance have been investigated as functions of feeding current density. The complex semiconductor structures may be recommend for the increase of a real time work period and the reliability of the power pulsed-mode diodes.

Keywords: Semiconductor Microwave Devices, Modeling and Simulation, Numerical Methods, Structure Optimization.

1 Introduction

One of the problems of high-power microwave semiconductor electronics is the design and construction of a generator with extraordinary energy characteristics. One of the solutions of this problem is to use pulsed-mode operation. The idea to use a special form of doping profile for the diode semiconductor structure has been realized in some works (El-Gabaly *et al.*, 1984; Chang, 1990; Zemliak and Roman, 1991; Curow, 1994; Tschernitz and Freyer, 1995). Modern semiconductor technology provides the possibilities for the fabrication of submicron structures with a complex doping profile. This gives one opportunity to design special IMPATT diode structures for pulsed-mode operation having high feed current values.

The main goal of the present project is analysis of the electrical and thermal processes of pulsed-mode high-power millimetric region IMPATT diode and the internal structure optimization to obtain the maximum output power and energy efficiency. In this work, the extreme energy characteristics of Si double-drift pulsed-mode IMPATT diodes for 94 GHz and for 140 GHz are investigated. The optimization of the internal structure of the diode with a traditional doping profile, (Fig. 1, curve 1) and with a complex doping profile (Fig. 1, curve 2) is provided.

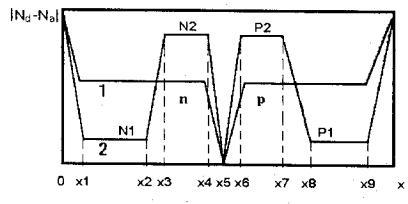

Figure 1. Doping profile for two types of IMPATT diodes: 1 - typical diode structure, 2 - complex diode structure x1,x2, ...,x9 are important technological lengths

We have marked special points of curve 2 on the longitudinal axis for the determination of different technological lengths that are independent parameters of the optimization procedure.

To investigate the physical processes and to optimize the internal diode structure we construct the new numerical model of the IMPATT diode in section 2 that provide the adequate accuracy and can reduce the total necessary computer time. The optimization procedure more suitable for the microwave device structure optimization is presented in section 3. The main results of the physical analysis and optimization are presented in section 4.

2 Numerical Model

The complex diode model consists of an electrical model that is based on the solution of the continuous equations system (1) jointly with one-dimensional Poisson equation and the thermal model that is based on the solution of heat-conductivity equation (2).

$$\frac{\partial n(x,t)}{\partial t} = \frac{\partial J_n(x,t)}{\partial x} + \alpha_n \left| J_n(x,t) \right| + \alpha_p \left| J_p(x,t) \right|$$
$$\frac{\partial p(x,t)}{\partial t} = -\frac{\partial J_p(x,t)}{\partial x} + \alpha_n \left| J_n(x,t) \right| + \alpha_p \left| J_p(x,t) \right| \qquad (1)$$

$$J_n(x,t) = n(x,t)\, V_n + D_n \frac{\partial n(x,t)}{\partial x}$$
$$J_p(x,t) = p(x,t)\, V_p - D_p \frac{\partial p(x,t)}{\partial x}$$
$$\frac{\partial T}{\partial t'} = \frac{k}{\rho C} \Delta T + \frac{1}{\rho C} Q\,(x,t',T) \qquad (2)$$

where Δ is the two-dimensional Laplace operator for the cylindrical coordinate system $\Delta T = \frac{\partial^2 T}{\partial x^2} + \frac{1}{r} \cdot \frac{\partial}{\partial r}\left(r \frac{\partial T}{\partial r} \right)$ r is the radial coordinate; x is the longitudinal coordinate; T is the Kelvin temperature; ρ is the material density; C is the specific thermocapacity; k is the thermoconductivity coefficient, and $Q\,(x,t',T)$ is the internal heat source that, in the general case, has a dependency on the electrical field, current density, and temperature.

Numerical solution of the main system (1) has been obtained by the modification of Crank-Nicolson numerical scheme that is the basis of the work (Zemliak *et. al.*, 1997), and that has a significant property of absolute stability as demonstrated in (Zemliak, 1981).

Numerical solution of equation (2) is performed by the iteration method of alternating directions. This model is different from the ones in (Kafka and Hess, 1981; Zemliak and Zinchenko, 1989; Dalle and Rolland, 1989; Stoiljkovic *et al.*, 1992; Vasilevskii, 1992; Tornblad *et al.*, 1996) because all electrophysical parameters are functions of the electric field and temperature at a corresponding point of the semiconductor structure, and because this model describes the heat source as a function of electric field intensity inside the diode structure.

One of the principal characteristics of the optimization procedure is the computer time for one probe of the objective function. Since one probe of the objective function includes the total analysis of the IMPATT diode, it is very important to reduce the complete diode analysis time. The complex diode model of the above mentioned paper (Zemliak *et. al.*, 1997) is based on the simultaneous use of electronic field and thermal models. This model has great accuracy, but is complicated too, and therefore its functioning is too slow for the optimization problem. In the present work we propose the model that uses the Fourier series analysis, and therefore has a limitation which is inherent in this technique. However, this model has a great advantage with its shorter computer time, and at the same time, it is a nonlinear model with sufficient accuracy. The other source of computer time reduction is the utilization of the high-order approximation numerical scheme for the thermal equation. These two ideas have been used successfully for the optimization of different types of IMPATT diodes.

The numerical method for the solution of the problem is based on classical Fourier series utilization. This method reduces the boundary problem for a system of differential partial equations to an ordinary differential equation's system. The new system describes physical processes in IMPATT diode in a stationary-operation mode. This method provides the possibilities to reduce the demands for a computer time that is necessary for the calculation of diode output parameters. Let us assume that all principal time-dependent functions of the system (1) can be presented in the form of a Fourier series:

$$n(x,t) = \sum_{m=-\infty}^{\infty} n_m(x) \cdot \exp(jm\omega t) \cdot \qquad (3)$$

In that case, the principal system (1) can be reduced to a system of ordinary differential equations for the complex charge density and for the current amplitudes:

$$\frac{dn_m}{dx} = \sum_{k=-\infty}^{\infty} \left\{ -\left(\frac{v_n}{d_n} \right)_k n_{m-k} + \frac{(I_n)_{m-k}}{(d_n)_k} \right\}$$
$$\frac{dp_m}{dx} = \sum_{k=-\infty}^{\infty} \left\{ \left(\frac{v_p}{d_p} \right)_k p_{m-k} - \frac{(I_p)_{m-k}}{(d_p)_k} \right\} \qquad (4)$$

$$\frac{d(I_n)_m}{dx} = jm\omega\ n_m - \sum_{k=-\infty}^{\infty}\{(\alpha_n)_k (I_n)_{m-k} + (\alpha_p)_k (I_p)_{m-k}\}$$

$$\frac{d(I_p)_m}{dx} = -jm\omega\ p_m + \sum_{k=-\infty}^{\infty}\{(\alpha_n)_k (I_n)_{m-k} + (\alpha_p)_k (I_p)_{m-k}\}$$

$$m = 0, \pm 1, \pm 2, ..., \pm\infty .$$

A number of harmonics m in these series can be reduced down to the number M, which defines the accuracy of the solution and necessary computer time. The system (4) can be presented in matrix form as

$$Y' = A\ Y . \tag{5}$$

The charge diffusion and sharp dependence of the ionization coefficients on the electrical field determine the great module of eigenvalues of the matrix A. For this case, a shooting method, which reduces the boundary problem to a Cauchy problem, is not suitable because the coordinate basis degenerates in the solution process, and therefore is not stable. The boundary problem (5) is solved on the basis of the functional matrix correlation as defined in the work (Krylov *et al.*, 1977):

$$B'(x)\ Y(x) = G(x) \tag{6}$$

where B' is the factorization matrix, and G is the boundary condition vector. The unknown matrixes of equation (6) are satisfied in the following differential equations' system:

$$\begin{aligned} B' + A' B &= 0 \\ G' &= 0 \end{aligned} \tag{7}$$

The fundamental matrix F is used to obtain the process stability of the integration of equations (7), This matrix is determined as $F(x) = \exp\{A'(x_k)h_k\}$, where h_k is the space step. Transition to the next coordinate node is made using the term $B(x_k + h_k) = F(x_k)\ B(x_k)$. The degradation of coordinate basis B can be overcome using Gram-Schmidt ortogonalization procedure for equation (6) at each integration step.

The algorithm for the analysis of the IMPATT diode includes the following steps: 1) the initial charge distribution of the diode is calculated; 2) the electric field harmonics are determined from the Poisson equation; 3) ionization and drift parameters and determined from the Fourier analysis, and the matrix of the system of equations on the coordinate net is formed; and 4) the boundary problem is solved for the system of continuity equations. Charge and current amplitudes are determined. The harmonics of the external circuit current are calculated. After this, the calculation cycle is repeated from the beginning to the point 2) until the external current is determined with sufficient convergence. Then all output parameters of the IMPATT diode are determined.

The IMPATT diode thermal model is based on the numerical solution of a nonlinear thermoconductivity equation (2) for silicon crystal, contact planes, and heat sinks. It determines the instantaneous semiconductor structure temperature at any point within the device for any given time moment. The thermal model that is described here has been utilized for the determination of temperature distribution in the diode structure having different types of doping profiles. The second order of the numerical approximation scheme for equation (2) is used often. In this case the alternating direction implicit method can be expressed in compact form as:

$$\frac{T_{ij}^{s+\frac{1}{2}} - T_{ij}^{s}}{\tau} = \frac{k}{\rho C}\left(\Lambda_1 T_{ij}^{s+\frac{1}{2}} + \Lambda_2 T_{ij}^{s}\right) + \frac{1}{\rho C} Q_j^{s}$$

$$\frac{T_{ij}^{s+1} - T_{ij}^{s+\frac{1}{2}}}{\tau} = \frac{k}{\rho C}\left(\Lambda_1 T_{ij}^{s+\frac{1}{2}} + \Lambda_2 T_{ij}^{s+1}\right) + \frac{1}{\rho C} Q_j^{s+\frac{1}{2}} \tag{8}$$

$$i = 1,2, ...I_2 - 1;\ \ j = 1,2,...J-1;\ \ s = 0,1,2,...\infty ;$$

where i, j are space coordinate numbers, s is the time coordinate number, Λ_1 is the partial numerical Laplace operator on the direction r, Λ_2 is the partial numerical Laplace operator on the direction x. Two of these operators are defined in the standard five-points numerical pattern: $\Lambda_1 T_{ij} = \frac{1}{h_1 i}\frac{T_{i+1,j} - T_{i-1,j}}{2h_1} + \frac{T_{i+1,j} - 2T_{i,j} + T_{i-1,j}}{h_1^2}$, $\Lambda_2 T_{ij} = \frac{T_{i,j+1} - 2T_{i,j} + T_{i,j-1}}{h_2^2}$. The numerical scheme (8) has the second approximation order only. In this case, it is necessary to develop the numerical net with a large number of cells to obtain sufficient accuracy. That is the reason why the total computer time that is necessary for the solution of the optimization problem is too great.

In this work, we propose the other type of thermal equation numerical approximation scheme for the acceleration of the thermal equation solution and for the reduction of the computer analysis time. The total analytic Laplace operator ΔT can be approximated with the numerical Laplace operator ΛT_{ij} as

$$\Lambda T_{ij} = \left(\Lambda_1 + \Lambda_2 + \frac{h_1^2 + h_2^2}{12}\Lambda_1\Lambda_2\right) T_{ij} \tag{9}$$

In that case, we can approximate the right part of equation (2) by the following numerical formula:

$$\frac{k}{\rho C}\Lambda T_{ij} + \frac{1}{\rho C}\left(E + \frac{h_2^2}{12}\Lambda_2\right) Q_j \tag{10}$$

where E is the identity operator.

The operator Λ is defined in the nine-point numerical pattern. The approximation (10) is more complicated, but it has the fourth approximation order. In that case, we can use the numerical net that is significantly more thin to obtain accuracy that is equal to the scheme (8) described above. For the solution of the principal equation (2) by approximations (9)-(10), we used one modification of the Peaceman-Rachford numerical scheme that had been developed by Samarsky (1968):

$$(E-k\cdot b\cdot(\tau-\chi_1)\Lambda_1)T_{ij}^{s+\frac{1}{2}} = (E+k\cdot b\cdot(\tau+\chi_2)\Lambda_2)T_{ij}^{s}+\tau\cdot b\cdot(E+\chi_2\Lambda_2)Q_j^s$$

$$(E-k\cdot b\cdot(\tau-\chi_2)\Lambda_2)T_{ij}^{s+1} = (E+k\cdot b\cdot(\tau+\chi_1)\Lambda_1)T_{ij}^{s+\frac{1}{2}}+\tau\cdot b\cdot(E+\chi_2\Lambda_2)Q_j^{s+\frac{1}{2}} \quad (11)$$

where $b=(1/\rho C)$, $\chi_{1,2}=(h_{1,2}^2/12)$.

We solve the system (11) by the tridiagonal algorithm for radial and longitudinal directions. This numerical scheme provides a significant gain of computer time in comparison with scheme (8).

3 Optimization Method

The optimization algorithm was designed as the combination of one of kind of direct method and a gradient method. This is one of the modifications of well-known algorithm, which is successfully used for function with complicate structures. This method is more precisely successful for the optimization of millimetric wave devices because the objective function of that type of device (for example, the output power) as a function of its arguments has a very complex behavior, similar to a one "valley" in N-dimensional space. The objective function can be determined as the maximum electronic power, for example.

The number of free variables for our case is equal to 8. These are four lengths *L1=x2-x1, L2=x4-x3, L3=x7-x6, L4=x9-x8* and four levels *N1, N2, P2, P1* of the diode doping profile. We have formed the principal vector of variables $y=\{y_1,y_2,y_3,y_4,y_5,y_6,y_7,y_8\}$ for these eight parameters of a semiconductor structure.

The optimization algorithm consists of the following steps: 1) Given as input two different approximations of two initial points: y^0 and y^1. 2) At these points, we start with the gradient method, and have performed some steps. As a result, we have two new points Y^0 and Y^1 that are determined by $y^{0n+1}=y^{0n}-\delta_n\cdot\nabla F(y^{0n})$, $y^{1n+1}=y^{1n}-\delta_n\cdot\nabla F(y^{1n})$, $n=0,1,\ldots N-1$, $Y^0=y^{0N}$, $Y^1=y^{1N}$, where F is the objective function, δ_n is the parameter of the gradient method. 3) We draw a line through two these points, and perform a large step along this line. We have a new point y^{s+1}: $y^{s+1}=Y^s+\alpha\left(Y^s-Y^{s-1}\right)$, $s=1$, where α is the parameter of the line step. 4) Than we perform a some steps from this point by the gradient method, and obtain a new point Y^s: $y^{s\,n+1}=y^{s\,n}-\delta_n\cdot\nabla F(y^{s\,n})$, $s=s+1$, $Y^s=y^{s\,N}$. Then steps 3 and 4 are repeated with the next values of the index s ($s=2, 3, \ldots$).

The optimization process that is presented above cannot find the global minimum of the objective function, but only a local one. To obtain the confidence that we have the better solution of the optimum procedure, it is necessary to investigate N-dimensional space with different initial points. In that case, it is possible to investigate N-dimensional volume in more detail. During the optimization process, it is very important to localize the subspace of the N-dimension optimization space for more detail analysis. The N-dimensional space volume of the independent parameters is determined approximately on the basis of model (4), (11) for the first stage of the optimization procedure. In that case, a Fourier series approximation of principal functions is used, and because of this approximate model, we have a ten times acceleration. After that, on the basis of the precise model, we have analyzed the internal structure of two types of silicon diode for 3 and 2 mm region. One of these structures is an ordinary constant doping profile structure, and the other is a complex one.

4 Results

The complex type of the double-drift IMPATT diode active layer is shown in Fig. 1, curve 2. The total width of the p-n junction was given as 0.15 μm and 0.12 μm for 94 GHz and for 140 GHz respectively. The doping profile gradients were determined by the lengths *x1*, *x3-x2*, *x8-x7*, which were selected as 0.075 μm and 0.06 μm for 94 GHz and for 140 GHz respectively. These values were given from the technological aspects, taking into account that the ion implantation technology is used. This is the approximation of the diode real doping profile, which can be produced in practice. This type of doping profile provides a concentration of electrical field within the p-n junction. On the other hand, for the diode with a permanent doping level, the following equalities are corrected: *N1=N2* and *P1=P2*. In that case, we have only four parameters for the optimization procedure: two lengths *L1=x4-x1*, *L2=x9-x6* and two doping levels *N1, P1*.

4.1 94 GHz Diode

In Fig.2 (a), (b) the characteristics of power-level and efficiency for the constant profile diode and complex profile diode for 94 GHz are presented as functions of feeding current density I_0 for the optimum structures and

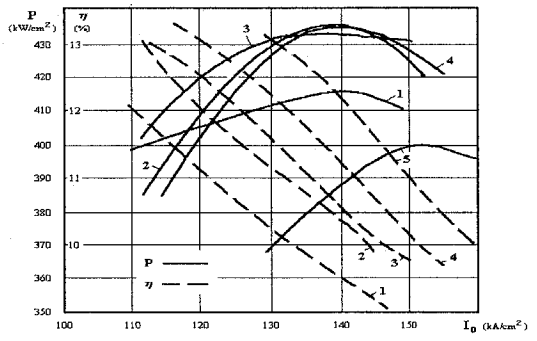

(a)

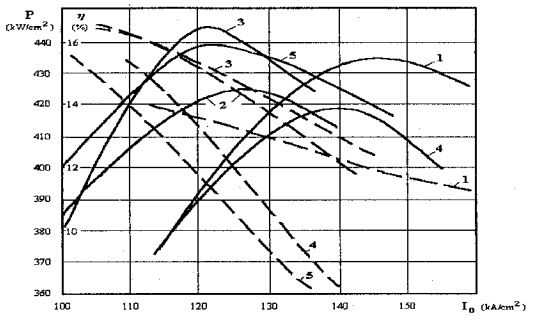

(b)

Figure 2. Output power P and efficiency coefficient η as functions of the feeding current density I_0 for optimum and near optimum structures for (a) constant and (b) complex doping profile diode

n	L1 (10^{-4} cm)	L2 (10^{-4} cm)	N1 (10^{17} cm^{-3})	P1 (10^{17} cm^{-3})
1	0.35	0.33	1.5	1.5
2	0.35	0.33	1.65	1.68
3	0.35	0.33	1.7	1.7
4	0.35	0.33	1.9	1.9
5	0.35	0.33	2.1	2.1

Table 1. Internal structure parameters for the diode with constant doping profile for 94 GHz

for others that are near the optimum. Parameters of these structures are presented in Table 1 and Table 2.

Structure 4 in Fig. 2(a) has the maximum power level 436 kW/cm^2 and the optimal current density value I_0=140 kA/cm^2. In that case, the efficiency is equal to 11.2 % for the maximum power point. Structure 5 has a maximum efficiency as the function of the current I_0, but for the optimum power point this value no larger than for structures 2, 3 and 4. Besides, for this structure it is necessary to increase the current value until 153 kA/cm^2 to obtain of the optimum power point.

Semiconductor structures with a complex doping profile are analyzed to improve of the power level and efficiency of pulsed-mode IMPATT diode (Fig. 2 (b)). In that case eight parameters have been varied: *L1, L2, L3, L4, N1, N2, P2, P1*. Structure 3 is the optimal one and has an efficiency of about 15% and 446 kW/cm^2 power level at 123 kA/cm^2. Others structures are near this optimum one but have a lower power level and efficiency. The extension of doping level high parts (structure 1) or increasing this level (structure 4) results to moving the power curve to the greater current density.

Comparison of the optimal characteristics for two different types of the structures as the constant doping profile (curve 4, Fig. 2a) and complex doping profile (curve 3, Fig. 2b) shows that the maximum output power level is almost equal for two these optimal structures (436 kW/cm^2 and 446 kW/cm^2), but efficiency coefficient has more difference (11.2% and 14.4%). The most important fact is a significant decrease of optimal value of permanent current density for the complex doping structure. The optimal current density value is equal to 140 kA/cm^2 for the constant doping structure, but for the complex doping structure is equal to 123 kA/cm^2. Therefore the complex doping profile structure has better energy characteristics.

4.2 140 GHz Diode

In Fig.3 (a), (b) the characteristics of power-level, efficiency, and the real and imaginary parts of the complex admittance of the 140 GHz diode are presented as functions of the feeding current density I_0 for the optimum structures and for others that are near the optimum. Parameters of the constant doping level and length values for this figure are presented in Table 3.

n	L1 (10^{-4} cm)	L2 (10^{-4} cm)	L3 (10^{-4} cm)	L4 (10^{-4} cm)	N1 (10^{17} cm^{-3})	N2 (10^{17} cm^{-3})	P2 (10^{17} cm^{-3})	P1 (10^{17} cm^{-3})
1	0.086	0.283	0.266	0.084	1.3	2	2	1.3
2	0.065	0.212	0.203	0.063	1.3	2	2	1.3
3	0.072	0.236	0.222	0.072	1.3	2	2	1.3
4	0.072	0.236	0.222	0.072	1.56	2.4	2.4	1.56
5	0.072	0.236	0.222	0.072	1.3	1.8	1.8	1.3

Table 2. Internal structure parameters for the diode with complex doping profile for 94 GHz

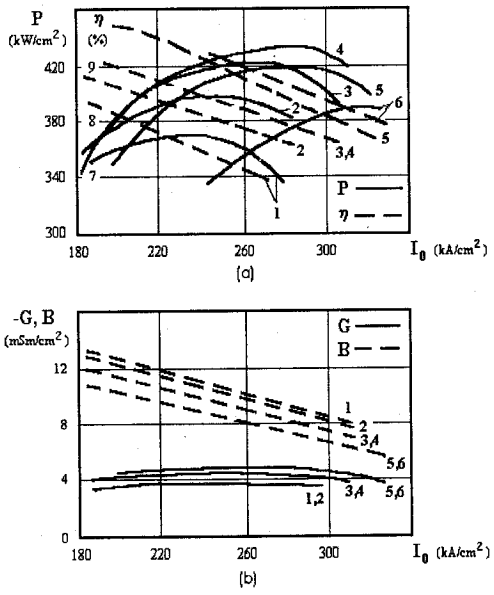

Figure 3. (a) Output power P and efficiency coefficient η, (b) real G and imaginary B parts of the total admittance as functions of feeding current density I_0 for optimal and near optimal structures with constant doping profile level

Structure 4 has a maximum power level of 430 kW/cm^2 and an optimal current density value of $I_0 = 285$ kA/cm^2. In that case, the efficiency is equal to 8.0 % for the maximum power point. Structure 5 has a maximum of the negative real admittance and efficiency (8.5 %), but has a smaller power level because the doping level is high, and therefore the permanent voltage and first harmonic amplitude voltage are smaller. Structure 6 has a maximum efficiency as the function of the current I_0, but for the optimum power point, this value is less than for structures 4 and 5. Besides, for this structure, it is necessary to increase the current value to 320 kA/cm^2 to obtain the optimum power point. Structures 5 and 6 have a maximum value of the real part of the total admittance, but have a greater doping level, and therefore a smaller value of the permanent and variable voltage and output power.

n	L1 (10^{-4} cm)	L2 (10^{-4} cm)	N1 (10^{17} cm^{-3})	P1 (10^{17} cm^{-3})
1	0.22	0.19	3	3
2	0.24	0.19	3.5	3.5
3	0.21	0.19	3.5	4.5
4	0.21	0.19	4	4
5	0.21	0.19	4.5	4.5
6	0.21	0.19	5	5

Table 3. Internal structure parameters for the diode with constant doping profile for 140 GHz

Semiconductor structures with a complex doping profile are analyzed for improving the power level and efficiency of the IMPATT diode with a maximum level of permanent current density. In Fig. 4 (a), (b) the dependencies of power level, efficiency and admittance are presented as functions of feeding current density I_0 for the optimum structure and for near optimum ones. Parameters of these structures are presented in Table 4.

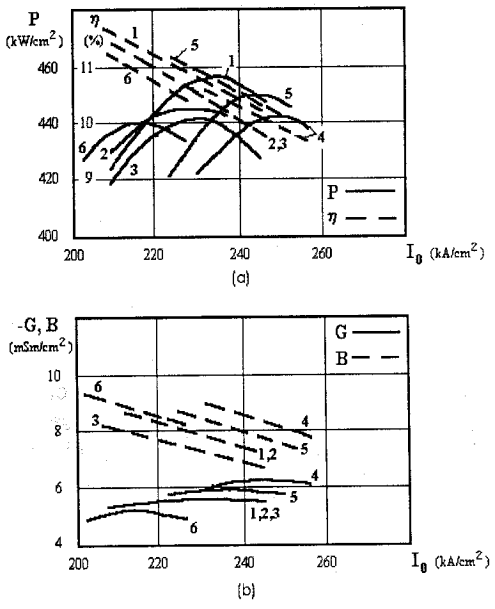

Figure 4. (a) Output power P and efficiency coefficient η and (b) real G and imaginary B parts of the total admittance as functions of feeding current density I_0 for optimal and near optimal structures with complex doping profile level

n	L1 (10^{-4} cm)	L2 (10^{-4} cm)	L3 (10^{-4} cm)	L4 (10^{-4} cm)	N1 (10^{17} cm^{-3})	N2 (10^{17} cm^{-3})	P2 (10^{17} cm^{-3})	P1 (10^{17} cm^{-3})
1	0.09	0.08	0.11	0.06	1.6	4.7	4.1	1.6
2	0.09	0.08	0.11	0.06	1.5	4.7	4.7	1.5
3	0.09	0.08	0.11	0.06	1.6	4.7	4.1	1.4
4	0.09	0.08	0.11	0.06	1.6	5.2	4.6	1.6
5	0.08	0.09	0.12	0.05	1.6	4.7	4.1	1.6
6	0.07	0.08	0.11	0.04	1.6	4.7	4.1	1.6

Table 4. Internal structure parameters for the diode with complex doping profile for 140 GHz

Structure 1 is the optimal one. In this case, the power level is 457 kW/cm^2, and the optimal current density value is 235 kA/cm^2. Others structures are near this optimum one, but have a lower power level and efficiency. The extension of the high doping level parts (structures 4 and 5) results in moving the power curve to a greater current density. These two types of semiconductor structures have a greater value of active admittance than the optimal one, but have a smaller microwave voltage amplitude and power level.

It is very important to compare the optimal characteristics for the two different types of structures as the constant doping profile (curve 4, Fig. 3(a)) and the complex doping profile (curve 1, Fig. 4(a)). A comparative analysis shows that the maximum output power level is almost equal for two these optimal structures (436 kW/cm^2 and 452 kW/cm^2), but the efficiency coefficient has more difference (8.5% and 10.7%). The most important fact is a significant decrease of the optimal value of the permanent current density for the complex doping structure. For the permanent doping structure, the optimal current density value is 285 kA/cm^2, but for the complex doping structure, it is 235 kA/cm^2. Therefore, the complex doping profile structure has better energy characteristics, and allows the possibility to exploiting the diode under easier conditions.

One of the important problems for the real type of the complex doping profile diode optimization is the sensitivity analysis of energy characteristics for various geometrical sizes and doping levels. The total number of the analyzed structures is very large, because of a large number of combinations of the 8 parameters. Some results of the investigation of an optimal structure by changing the doping profile levels *N1, N2, P2, P1* and lengths *L1, L2, L3, L4* within 20% around the optimal structure are presented in Tables 5 and 6, respectively. Presented examples give the possibility to evaluate correctly the technology inaccuracy influence to the energy characteristics deterioration. In these tables, we present the maximum achievable output power density, the permanent current density that corresponds to this optimum, and the real and imaginary parts of the complex admittance. The diode doping profile level increase within 20% with respect to the optimal structure leads to a small decrease of the output power. On the other hand, the diode doping profile level decrease leads to a great decrease of output power.

n	*N1* (10^{17} cm^{-3})	*N2* (10^{17} cm^{-3})	*P2* (10^{17} cm^{-3})	*P1* (10^{17} cm^{-3})	P_{max} (kW/cm^2)	I_{opt} (kA/cm^2)	*G* (mSm/cm^2)	*B* (mSm/cm^2)
1	1.6	4.7	4.1	1.6	455	235	-5.24	7.83
2	1.8	4.7	4.1	1.8	451	241	-5.36	7.51
3	2	4.7	4.1	2	451	242	-5.46	7.21
4	1.5	4.7	4.7	1.5	448	230	-5.25	7.51
5	1.4	4.1	4.1	1.4	443	227	-5.21	7.35
6	1.6	5	4.4	1.6	448	241	-5.71	8.07
7	1.6	5.2	4.6	1.6	447	251	-6.04	8.38
8	1.6	4.5	3.9	1.6	443	225	-4.78	8.51
9	1.6	4.2	3.7	1.6	440	227	-4.43	8.67

Table 5. Doping profile level variation within 20% around the optimal structure and diode output characteristics corresponding to these structures for 140 GHz

n	*L1* (10^{-4} *cm*)	*L2* (10^{-4} *cm*)	*L3* (10^{-4} *cm*)	*L4* (10^{-4} *cm*)	P_{max} (kW/cm^2)	I_{opt} (kA/cm^2)	*G* (mSm/cm^2)	*B* (mSm/cm^2)
1	0.09	0.08	0.11	0.06	455	235	-5.24	7.83
2	0.08	0.09	0.12	0.05	451	245	-5.51	7.91
3	0.07	0.1	0.13	0.04	447	253	-5.61	8.11
4	0.1	0.07	0.1	0.07	450	230	-4.97	8.11
5	0.11	0.06	0.09	0.08	445	225	-4.85	8.44
6	0.1	0.08	0.11	0.07	450	232	-5.17	7.41
7	0.11	0.08	0.11	0.08	447	234	-4.91	6.81
8	0.08	0.08	0.11	0.05	441	244	-5.34	7.41
9	0.07	0.08	0.11	0.04	434	246	-5.36	7.56

Table 6. Length variation within 20% around the optimal structure and diode output characteristics corresponding to these structures for 140 GHz

Some structures (6, 7 of Table 5) have a real admittance module greater than the optimal one (number 1), but because the microwave voltage amplitude is decreased, the output power level for these structures is smaller.

An analysis of the results that are presented in Table 6 shows that the variation of the total length $L=x9-x1$ around the optimal value leads to a great deterioration of the energy characteristics (structures 8 and 9). On the other hand, the redistribution of separate part's dimensions between the high and low doping profile parts within 20% has not led to a great decrease of the output power level.

5 Conclusions

Diode active layer optimization shows that the complex doping profile diode has a 6 % greater output power level and a 1.25-1.4 times greater efficiency coefficient with respect to the constant doping profile diode. This allows the possibility to obtain the maximum output power level with a smaller value of feed current density. The important feature of the optimal diode structure with a complex doping profile is a low sensitivity of the energy characteristics to the technological errors of the internal semiconductor structure. These complex semiconductor structures may be recommended for the increase of a real-time work period and the reliability of power pulsed-mode IMPATT diodes.

Acknowledgments

This research was supported by a CONACyT grant, number 28450A.

References

Chang K., *Handbook of Microwave and Optical Components,* Vol. 1, John Wiley & Sons, New York, 1990.

Curow M., "Proposed GaAs IMPATT Devices Structure for D-band Applications", *Electron. Lett.* Vol. 30, 1994, pp. 1629-1631.

Dalle C., and **P.A. Rolland,** "Drift-Diffusion Versus Energy Model for Millimetric-Wave IMPATT Diodes Modelling", *Int. J. Numer.Modelling*, Vol.2,1989, pp.61-73.

El-Gabaly M.A., R.K. Mains, and **G.I. Haddad**, "Effects of Doping Profile on GaAs Double-Drift IMPATT Diodes at 33 and 44 GHz Using the Energy-Momentum Transport Model", *IEEE Trans. Microwave Theory Tech.*, Vol. MTT-32, 1984, pp. 1353-1361.

Kafka H.J., and **K. Hess,** "A Carrier Temperature Model Simulation of a Double-Drift IMPATT Diode", *IEEE Trans. Electron Devices*, Vol. ED-28, 1981, pp. 831-834.

Krylov V.I., V.V. Bobkov, and **P.I. Monastyrski,** *Numerical Methods*, Nauka, Moscow, 1977.

Samarsky A.A., "About the choice of iteration parameters for the alternating direction method for Dirichlet high order accuracy differential problem", *Rep. Acad. Sci. USSR,* Vol.179, No.3, 1968, pp.548-554.

Stoiljkovic V., M.J. Howes, and **V. Postoyalko,** "Nonisothermal Drift-Diffusion Model of Avalanche Diodes", *J. Appl. Phys.,* Vol. 72, 1992, pp. 5493-5495.

Tornblad O., U. Lindefelt, and **B. Breitholtz,** "Heat Generation in Si Bipolar Power Devices: the Relative Importance of Various Contributions", *Solid State Electronics,* Vol. 39, No. 10, 1996, pp.1463-1471.

Tschernitz M., and **J. Freyer,** "140 GHz GaAs Double-Read IMPATT Diodes", *Electron. Lett.,*Vol. 31, No. 7, 1995, pp. 582-583.

Vasilevskii K.V., "Calculation of the Dynamic Characteristics of a Silicon Carbide IMPATT Diode", *Sov. Phys. Semicond.*, Vol. 26, 1992, pp. 994-999.

Zemliak A.M., "Difference Scheme Stability Analysis for IMPATT Diode Design", *Izvestiya VUZ Radioelectron.,* Vol. 24, No 8, 1981, pp. 88-89.

Zemliak A.M., and **S.A. Zinchenko,** "Non-linear Analysis of IMPATT Diodes", *Vestnik of the Kiev Polytech. Instit., Radiotechnika,* Vol. 26, 1989, pp. 10-14.

Zemliak A.M., and **A.E. Roman,** "IMPATT Diode for the Pulsed-Mode", *Izvestiya VUZ Radioelectron.,* Vol. 34, No. 10, 1991, pp.18-23.

Zemliak A., S. Khotiaintsev, and **C. Celaya,** "Complex Nonlinear Model for the Pulsed-Mode IMPATT Diode", *Instrumentation and Development,* Vol. 3, No. 8, 1997, pp. 45-52.

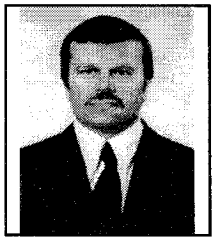

Alexander Zemliak, *received the M.S. and Ph.D. degrees from the Kiev Polytechnic Institute (KPI), Kiev, Ukraine, in 1972 and 1976, respectively, all in electronic engineering. From 1972 to 1976, he was a Researcher with the Department of Radio-Electronic Systems, KPI. From 1976 to 1994, he worked as a Professor at KPI. From 1994 he is a Professor of the Universidad Autónima de Puebla, Mexico. His research interests are in Computer-Aided RF and Microwave Circuit Analysis and Design, Analysis and Optimization of Microwave Devices.*

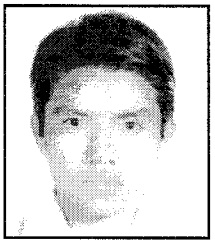

Roque De la Cruz Jiménez, *received the BSc degree in electronics in 1995 and his MSc degree in Optoelectronics in 1997 from Universidad Autónoma de Puebla. He is currently a PhD student in Optoelectronics. His research interest include Optoelectronics, Microwave and Millimeter Wave Simulation, Optical Simulation and Digital Image Processing.*